TAO, Vol.5, No.4, 463-475, December 1994

A New Strong-motion Array in Taiwan: SMART-2

HUNG-CHIE CHIU[1], YEONG TIEN YEH[1,2], SHEAN-DER NI[1],
LONG LEE[1], WEN-HSIANG LIU[1], GIN-FU WEN[1] and CHUN-CHI LIU[1]

(Manuscript received 27 May 1994, in final form 22 September 1994)

ABSTRACT

A new strong-motion array named SMART-2 has been deployed in the northern part of the Longitudinal Valley in Hualien, Taiwan. It consists of 40 free-field and 4 downhole-accelerometer stations (three in the Dahan Vertical Array and one in the Junkung Vertical Array). This array is designed mainly for the study of the rupture process of earthquake faulting and the characteristics of near-source ground motions. However, this high-quality (precise timing and high resolution) data set might be of further use in a variety of research areas both in Seismology and Earthquake Engineering.

Since the SMART-2 first started its operation, free-field stations have recorded 250 earthquakes with local magnitudes ranging from 2.5 to 6.1, and the Dahan Vertical Array has also recorded 51 earthquakes. In this paper, the authors present the status of the SMART-2 and some preliminary analyses of its data. Most of the SMART-2 stations are placed in firm gravel deposits. In a conventional broad classification, the site conditions of these stations may be classified into the same category; however, significant variations in ground motions across the array suggest that additional factors ought to be considered when classifying them. In addition to recording ground motions, the array can provide data to locate earthquakes. In this paper, it is shown that strong-motion array data can be a supplement to a regional network for locating earthquakes especially for those close to the array.

(Key words: Strong-motion array, SMART-2, Earthquake location)

1. INTRODUCTION

The dense strong-motion array observation program in Taiwan was started with the SMART-1 (Bolt *et al.*, 1982) in 1980. It was a two-dimensional surface array which included a center station $C00$, 36 stations on three concentric circles with radii of 200, 1000 and 2000 meters, and two stations in the extension arm. Except for station E02, all stations were

[1] Institute of Earth Sciences, Academia Sinica, P.O. BOX 1-55, Nankang, Taipei, Taiwan, R.O.C.

[2] Institute of Seismology, National Chung Cheng University, Minhsiung, Chiayi, Taiwan, R.O.C.

placed on alluvium sites. In 1985, the LSST (Large Scale Seismic Test) array (Tang *et al.*, 1988) was deployed inside the SMART-1 area to study soil-structure interaction. In that test program, a quarter and a 1/12 scaled nuclear containment model was constructed and instrumented with triaxial accelerometers. Besides the sensors installed on the structure, 15 free-field sensors were equally deployed on the three arms extending from the quarter scaled model, and a vertical array was also installed at both ends of one of these three arms. In all, there are a total of 14 triaxial accelerometers on the structure, 15 in the free-field on the surface and 8 in the downhole arrays.

After ten years of operating the SMART-1 array, the Second Workshop on Strong-Motion Array was held from January 14 to 16, 1988 in Taipei, Taiwan, Republic of China. The recommendations in this workshop initiated the second phase of the strong-motion dense array observation. It was suggested that a new strong-motion array on a firm-soil site in the Hualien area be installed to address some of the problems which had remained unsolved in the SMART-1 array and to make a comparison of these results with those from SMART-1. After the workshop, the Institute of Earth Sciences (IES) initiated a plan to deploy the second dense strong-motion array which was later named the SMART-2. In June 1990, the IES was then funded by Academia Sinica and the National Science Council, Republic of China to deploy a new array in the Hualien area within the following two to three years. Installation began in December 1990, and by the end of 1991 all 40 surface accelerographs were installed. Three borehole accelerographs were installed in April 1992, and the final borehole accelerograph was installed in August 1993. This paper describes the planning and current status of this new array. Likewise, some results from the analysis of the accelerograms recorded in the 23 January 1993 earthquake are included.

2. SELECTION OF SITES

The SMART-2 array was designed to study the source rupture process and near-source ground motions. For these purposes, the geological environment and seismicity were the greatest concerns in the selection of the sites. In both aspects, the Hualien area in eastern Taiwan was regarded as the most qualified site.

The eastern Taiwan area is situated on the juncture between the continental Eurasian Plate and the oceanic Philippine Plate. A linear and narrow fault-bounded Longitudinal Valley marks the collision suture of the two converging plates (Ho, 1982). Based on the distribution of hypocenters, Tsai (1978) pointed out the boundary bends along an east-west line at the latitude of 24°, and the plate subducts northward beneath the Ryukyu Arc. The Longitudinal Valley extends 150 km from Hualien to Taitung with a width of between 3 and 6 km and at an average of approximately 4 km. It lies between the Central Range and the Coastal Range.

The SMART-2 array is deployed on the northern part of the valley as shown in Figure 1. The geology of the SMART-2 array area and its vicinity is shown in Figure 2. The stations are located on either alluvium or terrace deposits. These two geological classes with similar depositional materials could be classified as having the same site conditions in the sense of broad geotechnical site classification. The terrain on the west side of the array is metamorphic rock of the Tananao Schist. To the east of the Longitudinal Valley, the Coastal Range is covered by Neogene and Quaternary pyroclastic and sedimentary sequences deposited in the intraarc basins of the Luzon-Taiwan volcanic arc (Wang *et al.*, 1991). The units based on the lithostratigraphic terms are Tuluanshan and Takangkou Formations.

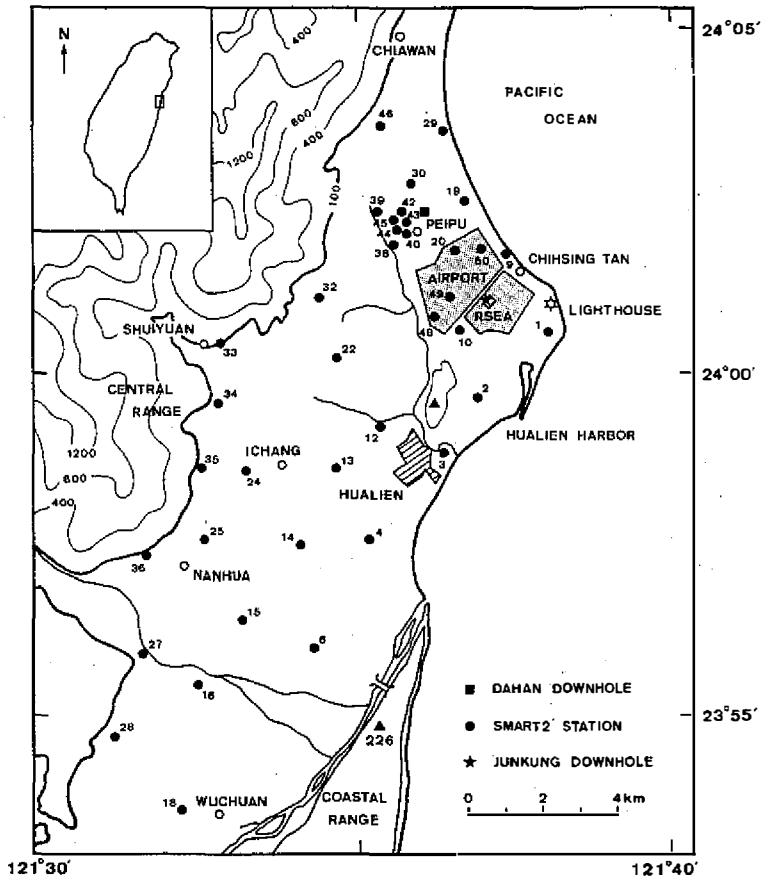

Fig. 1. The location and configuration of the SMART-2 array with its 40 free-field stations and two downhole vertical arrays. The last or the last two digits of each station's code are marked beside the surface stations.

Several geological features are related to the active seismicity in this region. The Meilun Fault strikes northeast and attains an observed length of about five kilometers. The Meilun Fault, surrounded by the SMART-2 array and considered to be related to the M=7.3 earthquake of October 22, 1951 (Hsu, 1962), is one of the major sources of high seismicity in the Hualien area. The faults along the boundary of the Longitudinal Valley and the nearby subduction boundary in the northeast of the array are also important sources of seismicity in this area. Consequently, the Hualien area is the most seismically active area in Taiwan. Within a circle of 60 km, with Hualien at the center, the annual number of earthquakes with a magnitude greater than 6 is 1, while those with a magnitude greater than 5.5 is 6.4. The most recent major event was in December 1990. Following its mainshock, there were several earthquakes with magnitudes greater than 5 to the south of the array. The largest event, M_L= 6.0, occurred on December 13, 1990, but at that time, only a few stations had been installed. Four days later, the IES sent out a team to deploy a temporary array of 15 stations to record the aftershocks. During a one-month period, about 400 earthquakes in all were recorded. This earthquake sequence demonstrates the great potential of the SMART-2 to record various types of near-source ground motions.

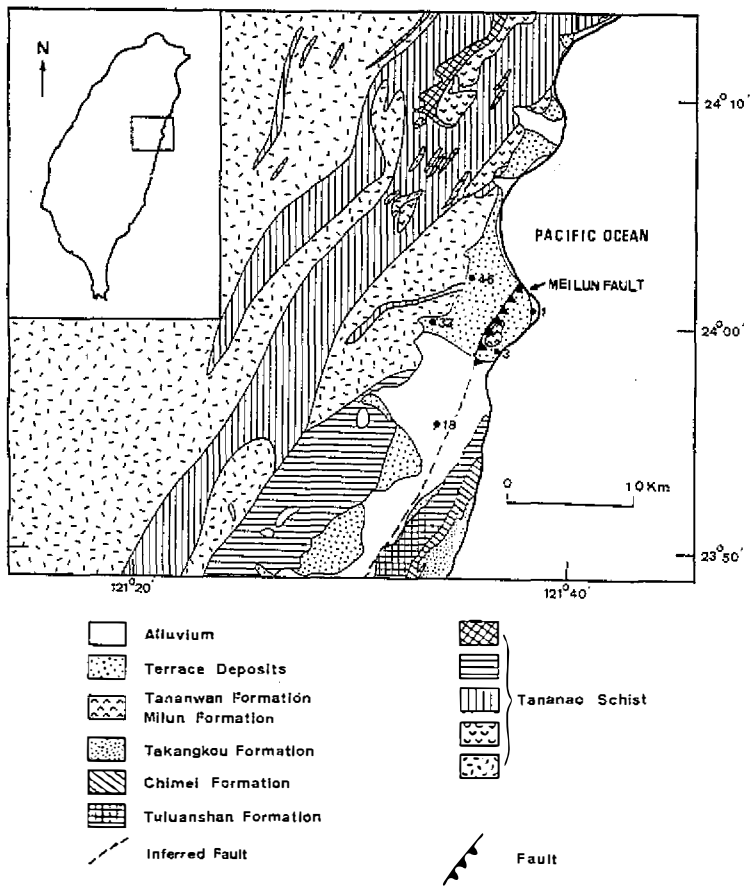

Fig. 2. The geological environment of the SMART-2 array and its vicinity with the Meilun Fault across the northern part of the array.

3. THE SMART-2 ARRAY

The SMART-2 array consists of 40 surface stations and two sets of downhole arrays. The surface configuration of the array is shown in Figure 1. Covering an area of about 110 km^2, these free-field stations are irregularly spaced approximately 2 km apart. Three downhole accelerometers were installed at depths of 50, 100 and 200 m in the Dahan Industrial School coincident with one of the free-field stations to form the Dahan Downhole Array. The other downhole accelerograph was installed at a depth of 100 m in the Junkung Marble Plant and is combined with 5 other shallow downhole accelerometers belonging to the Hualien LSST project to form one of the Junkung Downhole Arrays. Each free-field station includes a triaxial accelerometer, a SSR-1 recorder and an Omega receiver. For the vertical arrays, the same type of recorder is used, and all recorders in the same vertical array are connected to share common timing and triggering.

The deployment of these instruments started in December 1990 with most becoming operational by March 1991. By the end of 1991, 40 surface stations were deployed. The Dahan downhole array was installed in April 1992 while the Junkung downhole array was installed in August 1993. The locations of these stations (Table 1) had been carefully determined by a GPS survey which is accurate within a few meters.

Table 1. SMART-2 stations.

Code	Name	Latitude (N)	Longitude (E)	Elevation (m)
SM2001	Tai-Fei	24°00'26.71"	121°37'54.59"	5.80
SM2002	Mei-Lun Junior High School	23°59'59.60"	121°37'10.57"	24.24
SM2003	Hua-Gun Junior High School	23°58'41.24"	121°36'19.34"	19.37
SM2004	Nan-Hai	23°57'24.40"	121°35'12.71"	12.86
SM2006	Chung-Hua	23°55'52.40"	121°34'42.33"	23.97
SM2009	Chi-Hsing-Tan	24°01'45.33"	121°37'20.67"	11.74
SM2010	Hualien Normal University	24°00'34.84"	121°36'38.70"	14.37
SM2012	Hualien Agriculture and Technology School	23°59'09.64"	121°35'22.56"	13.67
SM2013	I-Chang Junior High School	23°58'24.22"	121°34'42.41"	20.61
SM2014	Tao-Hsiang	23°57'18.04"	121°34'09.72"	34.03
SM2015	Kuang-Hua	23°56'04.46"	121°33'30.59"	47.52
SM2016	Chung-Hsiao	23°55'11.80"	121°32'44.80"	53.16
SM2018	Wu-Chuan Elementary School	23°53'20.52"	121°32'22.97"	27.86
SM2019	Ku-Ching-Tou	24°02'33.57"	121°36'47.01"	17.09
SM2020	Hualien Airport	24°01'39.78"	121°36'19.81"	14.77
SM2022	Der-Hsing	24°00'09.32"	121°34'44.57"	25.88
SM2024	Fu-Hsing	23°58'25.39"	121°33'21.29"	40.54
SM2025	Nan-Hua	23°57'13.42"	121°32' 50.13"	63.28
SM2027	Mu-Kua-Hsi	23°55'41.38"	121°31'46.94"	73.64
SM2028	Chih-Hsueh	23°54'24.56"	121°31'27.31"	49.29
SM2029	Kang-Le	24°03'37.98"	121°36'20.96"	18.39
SM2030	Da-Hua	24°02'37.04"	121°35'52.14"	19.00
SM2032	Kuo-Fu	24°00'51.30"	121°34'09.95"	30.73
SM2033	Shui-Yuan Elementary School	24°00'18.12"	121°32'52.57"	80.94
SM2034	Tai-Chang	23°59'27.14"	121°32'40.90"	61.48
SM2035	San-Jou	23°58'29.24"	121°32'35.56"	57.14
SM2036	Kan-Cheng	23°57'14.99"	121°31'37.81"	91.17
SM2037	Pei-Pu (1)	24°02'17.55"	121°35'58.73"	18.79
SM2038	Pei-Pu (2)	24°01'46.94"	121°35'42.80"	16.80
SM2039	Pei-Pu (3)	24°02'19.89"	121°35'27.64"	22.13
SM2040	Pei-Pu (4)	24°02'00.15"	121°35'51.99"	19.90
SM2042	Pei-Pu (5)	24°02'17.68"	121°35'46.37"	21.19
SM2043	Pei-Pu (6)	24°02'10.36"	121°35'48.97"	20.21
SM2044	Pei-Pu (7)	24°02'04.74"	121°35'45.13"	21.35
SM2045	Pei-Pu (8)	24°02'11.35"	121°35'41.23"	23.24
SM2046	Chia-Min	24°03'43.83"	121°35'27.65"	32.40
SM2048	Air Force (South)	24°00'45.63"	121°36'18.34"	11.88
SM2049	Air Force (center)	24°01'14.41"	121°36'35.05"	10.47
SM2050	Air Force (North)	24°02'05.24"	121°37'00.31"	14.85
DHD001	Dahan Downhole (surface)	24°02'22.12"	121°36'04.04"	18.33
DHD002	Dahan Downhole (50m)	24°02'22.12"	121°36'04.04"	
DHD003	Dahan Downhole (100m)	24°02'22.12"	121°36'04.04"	
DHD004	Dahan Downhole (200m)	24°02'22.12"	121°36'04.04"	
JKD 001	Junkung Downhole (100m)	24°01'01.27"	121°37'40.70"	

Most of the fault systems in the Hualien area are parallel to the Longitudinal Valley. To study the rupture process of earthquake faulting, controls in both parallel (strike slip) and perpendicular (dip slip) directions were required. The configuration of the SMART-2 (Figure 2) was, therefore, designed to meet these requirements. More densely installed stations and two downhole arrays were positioned in the northern part of the SMART-2 array. The dense stations and the Dahan Downhole Array (see Chiu *et al.*, 1994) were deployed on the west side of the Meilun Fault (Figure 2) whereas the Junkung Downhole Array was installed on the east side of the fault. These subarrays were designed to study not only the spatial variation of ground motion in a small region but also the site response.

In the initial design, the distribution of free-field stations was more uniform than in the current configuration. The locations of these stations were later adjusted to meet the site conditions and the availability of lands. However, the same station codes used in the planning stage have been kept. Consequently, some numbers are missing in the current station codes (Table 1 and Figure 1).

4. INSTRUMENTATION

Each free-field station in the SMART-2 array consists of a FBA-23 sensor, a SSR-1 digital recorder and an Omega antenna. The features of these instruments are explained below.

4.1 Sensors

Kinemetrics' triaxial force-balance accelerometers, the FBA-23's, are used at free-field stations and FBA-23DH's at downhole stations. Most of these sensors have a full scale of 1g but a few have 2g. The dynamic range of the sensors is 140db. Their natural frequency is 50 Hz, and damping is 70% of critical damping. Each sensor has a very flat frequency response from DC to about 20 Hz. After instrument correction, these data can extend reliable signals up to 50 Hz. This band width is adequate for earthquake rupture and near-source ground-motion studies. The longitudinal axis of each sensor is set to point north.

4.2 Recording and Timing Systems

A recording and timing unit consists of a Kinemetrics' SSR-1 recorder and an Omega clock. These recorders have a 16-bit resolution which is equivalent to a 0.0305 gal/count for 1g sensors. The Omega clock provides a relative timing accuracy of about one millisecond between any two strong-motion stations. Such accuracy is maintained by having the clocks continuously synchronized with the time of the standard station in Japan.

The ground motions sensed from accelerometers are converted to digital voltage and are stored in solid-state memory. A typical RAM memory is 2 megabytes which can record 27 minutes of three-component records for a 200 sampling rate recording.

This recorder also provides adjustable pre-event and post-event memory. In the SMART-2 array, 10 seconds for pre-event memory and 30 seconds for post-event memory are programed. At best, this pre-event memory ensures that the first P-arrival is well recorded.

For the trigger algorithm, a band-pass filtered threshold was selected. Although the setting of the level of threshold depends on the background noise of the individual station, the typical threshold is about 5 gal. Each of the three accelerometers can be treated as an independent trigger having one vote for the more advanced setting of the triggering. This

recorder also allows for the use of a number of total votes to make the triggering even more flexible. By requiring more than one vote to trigger the recorder, false triggering caused by single component noise spikes can be avoided. For the SMART-2 array, the typical vote set is 1, the value at which the recording unit starts when any component of ground motion reaches the threshold. Once the ground motions drop below this level, the recording system lasts for a period which is set as the post-event hold time, and then it returns to its stand-by status.

4.3 Shelters for Instruments

A typical station in the SMART-2 array consists of 125 cm×125 cm×10 cm concrete pads and a fiberglass hut which provides shelter for the accelerometer and recorder. The accelerometer is bolted near the center of the pad. The coupling between the concrete pad and the ground is enhanced by four 75-cm stainless steel sticks. One end of these sticks is cemented into the pad while the rest of them penetrate into the ground.

4.4 Antennae of the Omega Clocks

The antennae of the Omega clocks are erected beside the fiberglass huts. In most instances, the antenna poles are extended to a higher position to enable a better reception of the time signals.

5. PRELIMINARY ANALYSES OF DATA

The earthquake data in the SSR-1 recorder are stored in a binary form. In the field, these data are retrieved and stored in a portable personal computer. In the laboratory, these binary data are changed into easy-to-read formats and are converted from voltage to ground acceleration. Since the first installation in 1990, this array has recorded 250 earthquakes, the epicenters of which are shown in Figure 3. The local magnitudes of these earthquakes range from 2.5 to 6.1.

With one filtering plus two least-square fittings, the baseline of the integrated displacement time histories can be corrected well. Eight EW-component displacement time histories are shown in Figure 4. Unreasonable offsets before or after the seismic signals do not appear in these displacement time histories. Since the high-resolution digital data reduce many sources of errors which may exist in conventional strong-motion data, the frequency range of the reliable signal should be wider than that of the conventional data. To retrieve more information from the strong-motion accelerograms, it is necessary, therefore, to develop a new processing algorithm for high-resolution data.

The EW-component accelerations corresponding to Figure 4 are used to calculate the response spectra over 90 periods ranging from 0.01 to 30 seconds. The tripartite logarithmic plot of pseudo velocity for 5 damping values are given in Figure 5. The values at long- and short-period ends should asymptotically approach the peak ground displacement and acceleration, respectively. It is well known that the long-period portion of the response spectra are very sensitive to noise. Therefore, if the acceleration is contaminated by noise, the long-period response spectra will deviate from the line corresponding to the peak ground displacement. As shown in Figure 5, all these data have a very good approximation to the asymptotical lines.

With the accurate timing, it is possible to use these strong-motion data to relocate the hypocenters. The characteristics of high-resolution, three-component data and the on-scaled

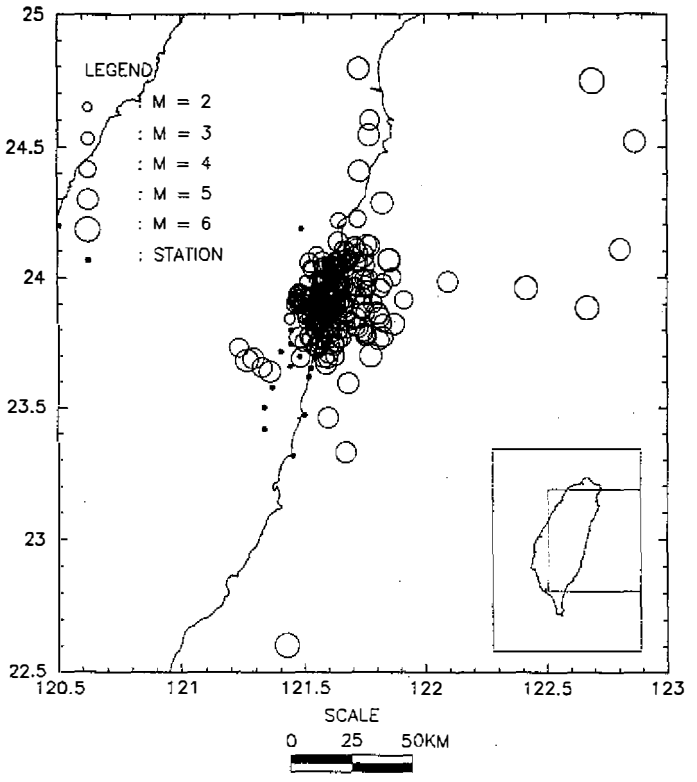

Fig. 3. The epicentral map of SMART-2 data (Dec. 1990 - Apr. 1994). The SMART-2 and its temporary stations are shown by small solid circles. The epicenters are shown by open circles and the size of the circle is proportional to the size of the earthquake.

recording are helpful for the picking of arrival. First, the time and amplitude scales of the high resolution digital data can be easily expanded to allow the precise picking of arrival times. Second, three-component data can be properly rotated to enhance the primary S arrival. Finally, the large dynamic range allows the completed waveform to be recorded on-scale. The latter two features are especially important in identifying S arrivals.

The earthquake on January 23, 1993 triggered 30 SMART-2 accelerographs. A subset of the East-West component of these accelerograms is plotted according to their epicenter distances (Figure 6). The picked P and S arrivals are marked by arrows, and the predicted arrivals calculated from the relocation are marked by crosses. Mostly, the picked arrivals are very close to the calculated arrivals. This earthquake, as located by the local network, was offshore and northeast of the array. After relocation using the SMART-2 data, it is evident that the new epicenter was inland and northwest of the array. The contour of relative P arrival time (Figure 7) also indicates that the direct P waves came from a northwestern direction.

Most of the SMART-2 stations lie on a deep gravel deposit which can be classified as having the same site conditions in the sense of a broad classification. If the site amplifications are similar within the array, the contour of peak ground accelerations (PGA's) should be more or less similar to the pattern of P arrival time. However, the observed ground motions show an evident spatial variation. One example of the large spatial variation of the PGA's is given

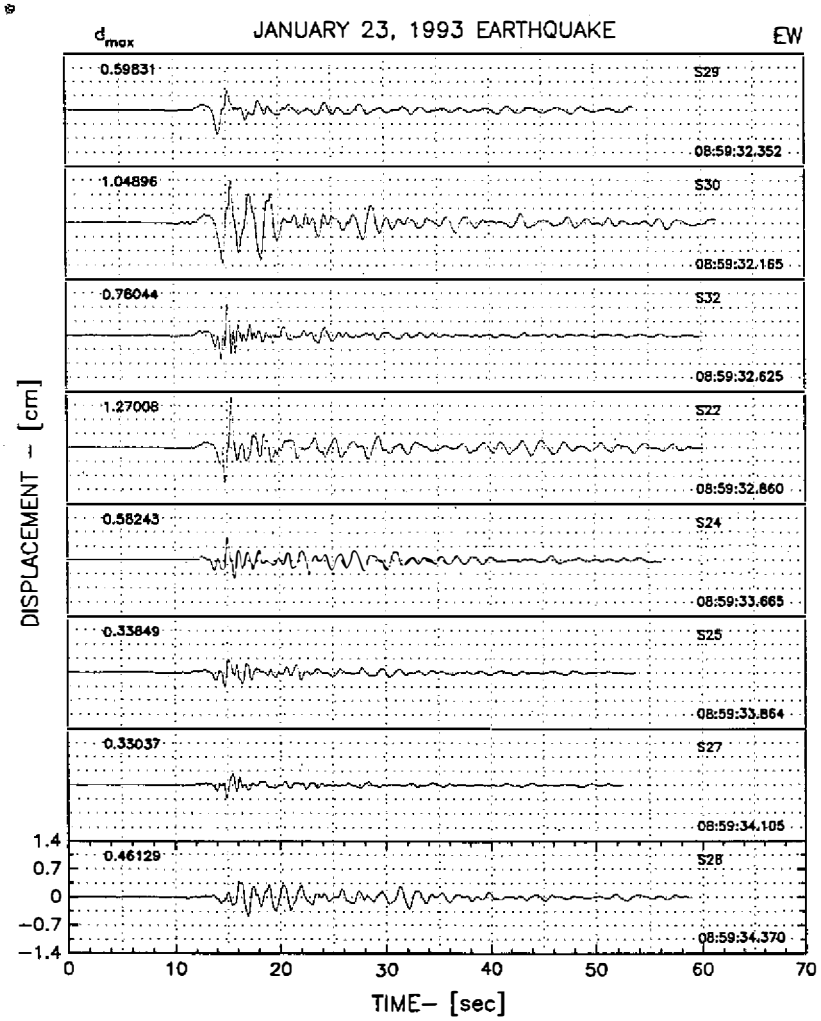

Fig. 4. The integrated ground displacements from eight EW-component accelerograms during the January 23, 1993 earthquake.

in the contour plot as shown in Figure 8. There are relative highs at station S19 and in the dense array region around station S39, and a relative low around stations S27 and S15. This pattern varies for different events which implies that site effects are complicated and a large variability of site amplification can still be found in those stations within the same broad classification.

6. CONCLUSIONS

The SMART-2 array in Hualien has provided a high-quality data base for studying earthquake source and near-field ground motions and is expected to have great potential for recording various types earthquakes with different magnitude, epicenter distance or focal mechanism.

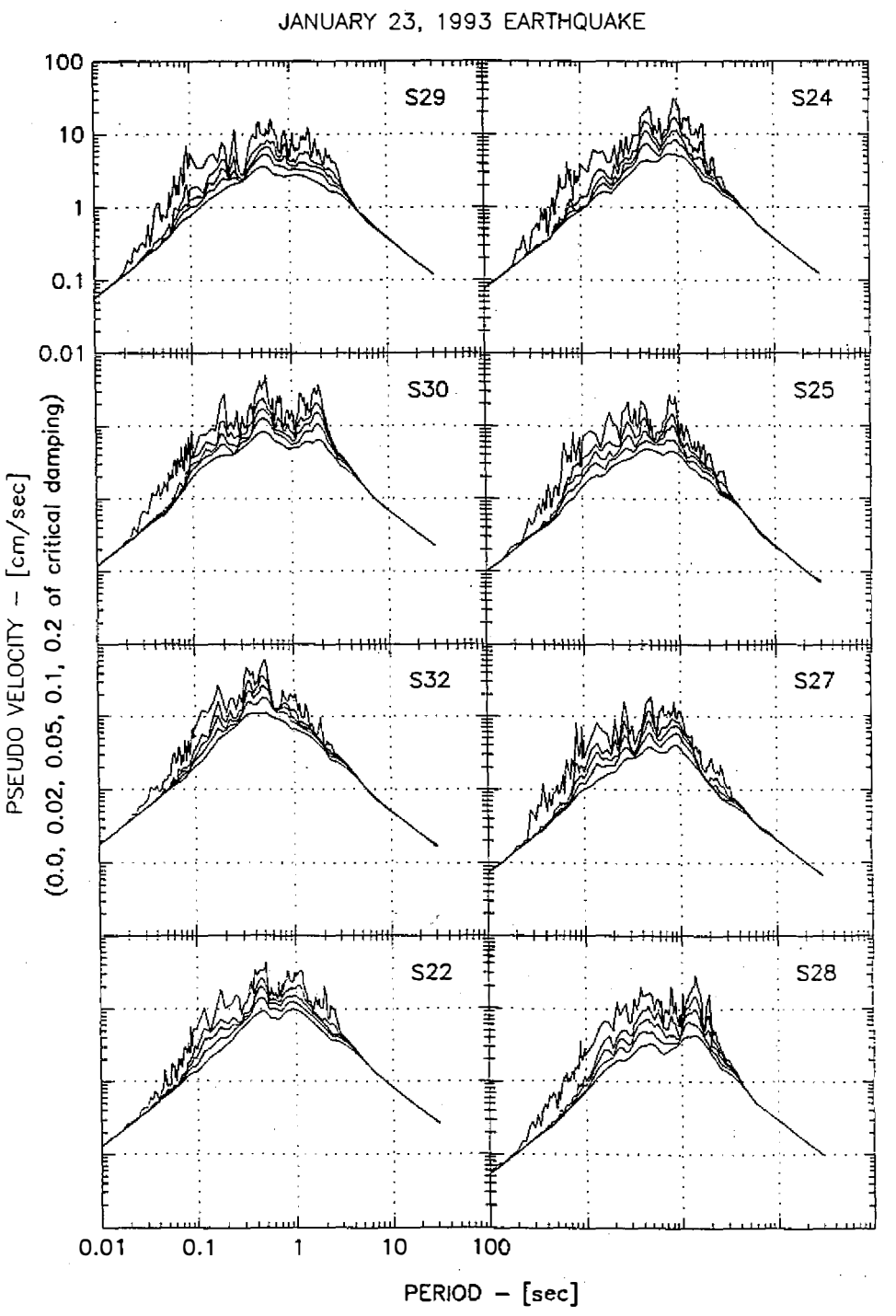

Fig. 5. The tripartite logarithmic plots of the pseudo velocities of the eight EW-component accelerograms of the January 23, 1993 earthquake.

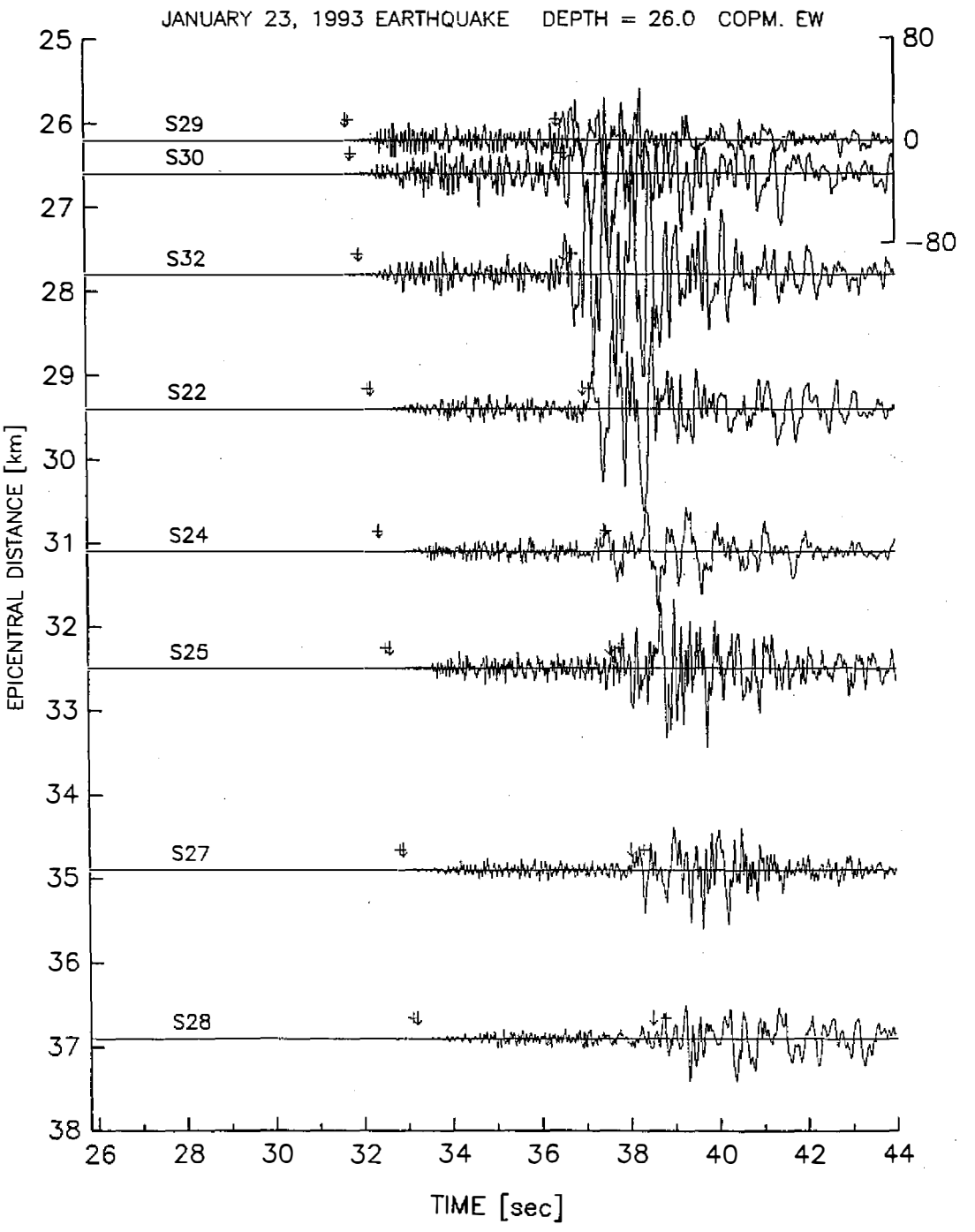

Fig. 6. Some selected EW-component accelerograms according to their epicentral distances. The picked P and S arrivals are marked by arrows and the calculated arrivals are marked by crosses.

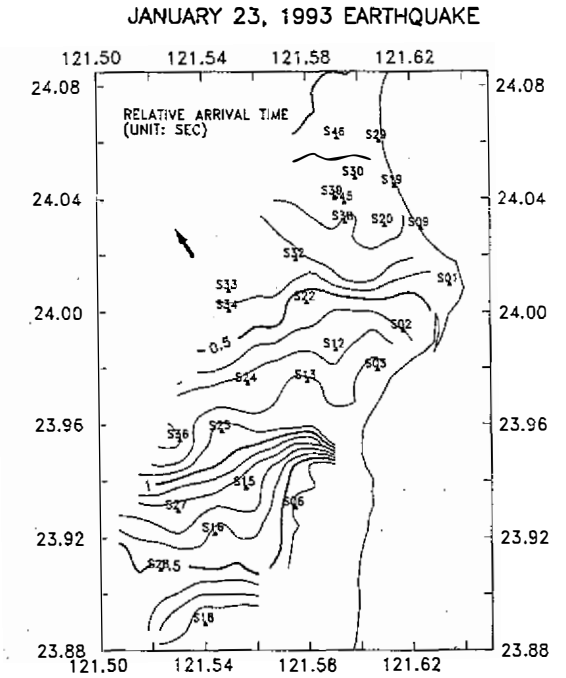

Fig. 7. The contour of the primary P arrival times for the January 23, 1993 earthquake. The arrow in the upper left corner points to the epicenter which is 26.6 km away from station S33.

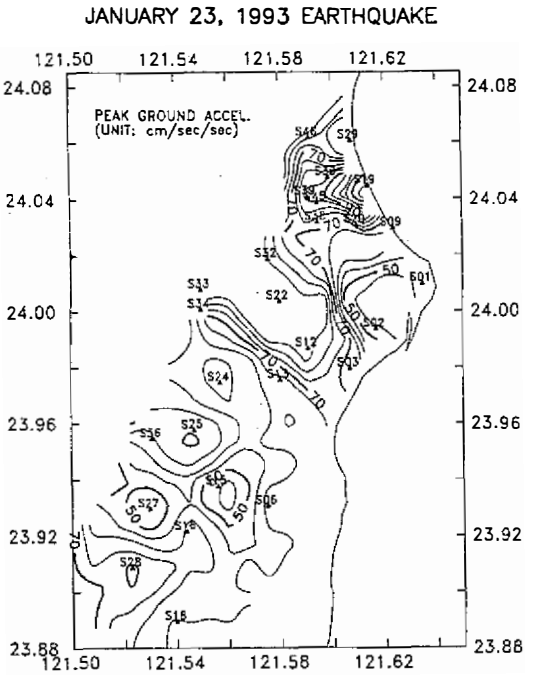

Fig. 8. The contour of the PGA's for the January 23, 1993 earthquake.

The quality of 16-bit data is much better than the conventional strong-motion data (analog data or 12-bit recordings). With minimal processing, both the integrated displacements and the response spectra can be accurately calculated. Nevertheless, further study is still necessary to develop a new algorithm for data processing to retrieve more information from these 16-bit or higher resolution data.

The improvement of timing and the resolution of strong motion data render the differences between a strong-motion network and a local network smaller and smaller. Consequently, it is possible to merge these two types of networks into a hybrid network using high-resolution accelerometers. This hybrid network might meet the requirements of both types of array. In any case, SMART-2 has shown itself to be a satisfactory supplementary network for earthquake location in the Hualien area.

Acknowledgments The authors gratefully acknowledge the help of various individuals and organizations during the deployment of the array. The precise locations of the stations were measured by colleague, Dr. S. B. Yu, and his GPS team which is most appreciated. The authors are also grateful for the many helpful suggestions received from Drs. B. A. Bolt, T. L. Teng, Y. B. Tsai, F. Wu and W. H. K. Lee, during the planning, deployment and operation of the SMART-2 array. The authors thank Dr. N. A. Abrahamson for many well-made suggestions on the manuscript. The research was supported by Academia Sinica and the National Science Council under contracts NSC-79-0202-M001-27, NSC-81-0202-M001-03 and NSC-82-0202-M001-095.

REFERENCES

Bolt, B. A., Y. B. Tsai, K. Yeh, and M. K. Hsu, 1982: Earthquake strong motions recorded by a large near-source array of digital seismographs. *Earthq. Eng. Struct. Dyn.*, **10**, 561-573.

Chiu, H. C., H. C. Huang, C. L. Leu, and S. D. Ni, 1994: Application of polarization analysis in correcting the orientation error of a downhole seismometer. *Earthq. Eng. Struct. Dyn.*, (In press)

Ho, C. S., 1982: Tectonic evolution of Taiwan: explanatory text of the tectonic map of Taiwan. The Ministry of Economic Affairs, Republic of China, 126pp.

Hsu, T. L., 1962: Recent faulting in the Longitudinal Valley of eastern Taiwan. *Memo. Geol. Soc. China*, **1**, 95-102.

Tang, H. T., Y. K. Tang, J. C. Stepp, I. W. Wall, E. Lin, S. C. Cheng, H. N. Hsiao, and S. K. Lee, 1988: A large-scale soil-structure interaction experiment: design and construction. Proc. The Second Workshop on Strong Motion Arrays, Taipei, Taiwan, Republic of China.

Tsai, Y. B., 1978: Plate subduction and the Plio-Pleistocene orogeny in Taiwan, *Petrol. Geol. Taiwan*, **15**, 1-10.

Wang, Y., C. N. Yang, and W. S. Chen, 1991: Explanatory text of the geological map of Taiwan, Sheet 35 (Hualien). Central Geological Survey, Republic of China, 55pp.